Multipartite Entanglement in Topological Quantum Phases

Luca Pezzè,[1] Marco Gabbrielli,[1,2] Luca Lepori,[3,4] and Augusto Smerzi[1]

[1]*QSTAR and INO-CNR and LENS, Largo Enrico Fermi 2, 50125 Firenze, Italy*

[2]*Dipartimento di Fisica e Astronomia, Università degli Studi di Firenze, via Sansone 1, I-50019 Sesto Fiorentino, Italy*

[3]*Dipartimento di Scienze Fisiche e Chimiche, Università dell'Aquila, via Vetoio 42, I-67010 Coppito-L'Aquila, Italy*

[4]*INFN, Laboratori Nazionali del Gran Sasso, Via G. Acitelli 22, I-67100 Assergi (AQ), Italy*

(Received 4 July 2017; revised manuscript received 5 October 2017; published 18 December 2017)

We witness multipartite entanglement in the ground state of the Kitaev chain—a benchmark model of a one dimensional topological superconductor—also with variable-range pairing, using the quantum Fisher information. Phases having a finite winding number, for both short- and long-range pairing, are characterized by a power-law diverging finite-size scaling of multipartite entanglement. Moreover, the occurring quantum phase transitions are sharply marked by the divergence of the derivative of the quantum Fisher information, even in the absence of a closing energy gap.

DOI: 10.1103/PhysRevLett.119.250401

Introduction.—The characterization of quantum phases and quantum phase transitions (QPTs) via entanglement measures and witnesses is an intriguing problem at the verge of quantum information and many-body physics [1,2]. The study of entanglement [3,4] pushes our understanding of QPTs [5–8] beyond standard approaches in statistical mechanics [9] and sheds new light on the creation, manipulation, and protection of useful resources for quantum technologies.

The literature [1] has mostly focused on bipartite entanglement. A benchmark is the so-called area law [10–12] that relates the amount of entanglement among two parts of a many-body system to the surface area between them [13,14]. For models with short-range interaction in one dimension, the von Neumann block entropy is constant in the gapped phases, while it increases logarithmically with the system size at criticality [15]. Yet, violations of the area law are not always related to a closing gap: A logarithmic increase of the von Neumann entropy occurs also in some gapped phases of one-dimensional models with long-range interaction [16–19], as well as for peculiar short-range models [20]. An alternative approach to bipartite entanglement is the analysis of the two-body reduced density matrix [7,21], often also indicated as pairwise entanglement.

Multipartite entanglement (ME) allows us to disclose the richer and more complex structures of a many-body quantum system [4]. However, ME can be more difficult to evaluate than bipartite entanglement and has been much less studied [22–24]. Recently [25–27], ME in the ground state of models exhibiting symmetry-breaking QPTs has been witnessed using the quantum Fisher information (QFI) calculated for the local order parameter. In this case, the QFI—given by the variance of the order parameter—diverges (in the thermodynamic limit) at criticality. Exploiting well-known relations between the QFI and ME [28–31], it has been possible to witness large ME in spin systems, such as the Ising [25], *XY* [26], and the Lipkin-Meshkov-Glick [25,27] model. This approach, however, fails to detect ME at topological QPTs [25], where the fluctuations of local operators do not diverge at criticality [32]. Witnessing ME in topological models using the QFI generally require the extension of entanglement criteria for nonlocal operators [31].

Here we focus on a paradigmatic model showing topological quantum phases: the Kitaev chain of spinless fermions in a lattice [33,34] with variable-range pairing [17,19,35]. We calculate the QFI of the ground state for a suitable choice of nonlocal observables and witness ME (the parties being the single sites of the chain) when the corresponding correlation functions have a sufficiently slow decay. We show that phases identified by a nonzero winding number are characterized by a superextensive scaling of the QFI, signaling the divergence of ME with the system size. This divergence is found, for short-range pairing, only at topologically nontrivial phases, hosting massless edge modes. Instead, for long-range pairing, superextensivity of the QFI is found whenever the winding number assumes semi-integer values. Furthermore, for an arbitrary pairing range, ME is shown to vary suddenly at QPTs, even when the energy gap in the quasiparticle spectrum does not close at the boundary lines. Overall, ME provides more information than that caught by the von Neumann entropy [17–19], not able to discern between the phases with different winding numbers of the short-range or the long-range regime and just detecting the separation lines between them. Our work addresses an open problem in the literature—the detection of ME in topological phases and QPTs—and paves the way towards a characterization of strongly correlated systems in terms of ME.

The model.—The Kitaev chain is a tight-binding model with both tunneling and superconducting pairing. This was

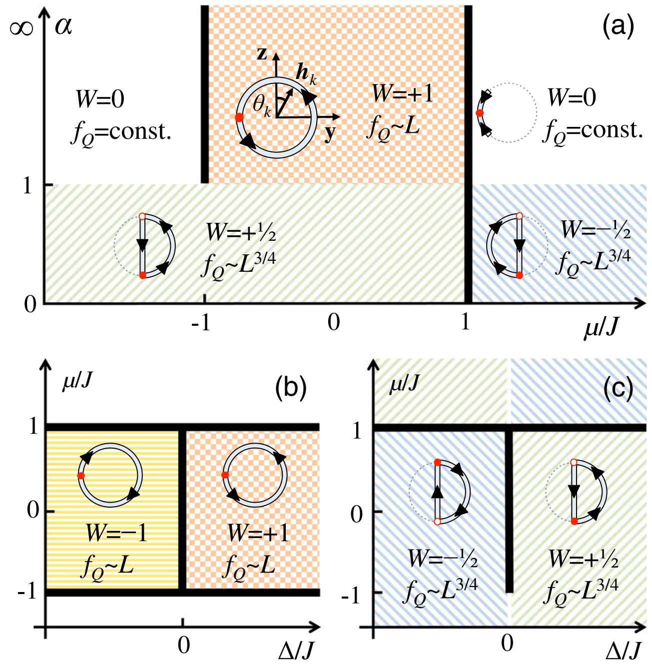

FIG. 1. Phase diagram of the Kitaev chain in the $\mu/J-\alpha$ plane for $\Delta>0$ [38] (a). Phase diagram in the $\Delta/J-\mu/J$ plane for (b) nearest-neighbor ($\alpha=+\infty$) and (c) infinite-range ($\alpha=0$) pairing. The thick lines mark a closing gap in the quasiparticle spectrum [Eq. (2)] in the thermodynamic limit $L\to\infty$. Colored regions highlight different phases with indicated winding number W and scaling of the Fisher density $f_Q=F_Q/L$ with the system size L. Thick curved lines show trajectories in the unit circle in the y-z plane (dotted line) as k varies from 0 (red dot) to 2π (red circle); see the text.

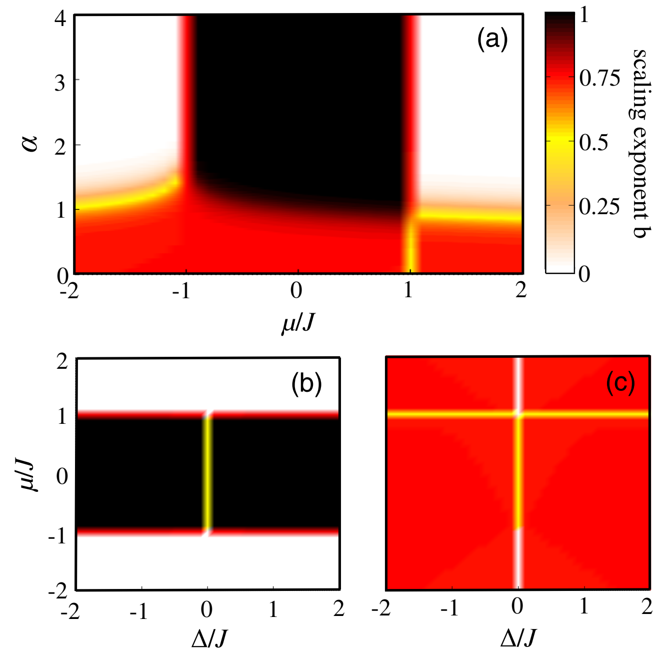

FIG. 2. Phase diagram of the Kitaev chain obtained numerically from the scaling of the Fisher density as a function of the system size L, $f_Q=1+cL^b$ [Eq. (5)]. The color scale shows the scaling exponent b in the $\mu/J-\alpha$ plane for $\Delta=J$ (a) and in the $\Delta/J-\mu/J$ plane for nearest-neighbor (b) and infinite-range (c) pairing.

originally studied for nearest-neighbor pairing [33] and extended to variable-range pairing in Refs. [17,19]. The corresponding Hamiltonian is

$$\hat{H}=-\frac{J}{2}\sum_{j=1}^{L}(\hat{a}_j^\dagger\hat{a}_{j+1}+\mathrm{H.c.})-\mu\sum_{j=1}^{L}\left(\hat{a}_j^\dagger\hat{a}_j-\frac{1}{2}\right)+\frac{\Delta}{2}\sum_{j=1}^{L}\sum_{\ell=1}^{L-j}\frac{1}{d_\ell^\alpha}(\hat{a}_j\hat{a}_{j+\ell}+\hat{a}_{j+\ell}^\dagger\hat{a}_j^\dagger),\quad(1)$$

where $J>0$ is the hopping amplitude, Δ is the pairing strength, μ is the chemical potential, and L (assumed even) is the total number of lattice sites. The operator $\hat{a}_j$ ($\hat{a}_j^\dagger$) annihilates (creates) a fermion at site j. We consider a closed chain, with $d_\ell=\ell$ for $1\le\ell\le L/2$ and $d_\ell=L-\ell$ for $L/2\le\ell<L$, and antiperiodic boundary conditions $\hat{a}_{j+L}=-\hat{a}_j$. Following Ref. [36], the Hamiltonian (1) can be diagonalized exactly by a Bogoliubov transformation. The resulting quasiparticle spectrum is [17,37]

$$\epsilon_k=\sqrt{(J\cos k+\mu)^2+[f_\alpha(k)\Delta/2]^2},\quad(2)$$

where $k=(2\pi/L)(n+\frac{1}{2})$ ($n=0,1,\ldots,L-1$). The function $f_\alpha(k)=\sum_{\ell=1}^{L-1}(\sin(k\ell)/d_\ell^\alpha)$ displays singularities at $k=0$ in the thermodynamic limit if $\alpha\le1$; it is regular otherwise. Taking the Fourier transform, Eq. (1) becomes $\hat{H}=\sum_k\epsilon_k(\hat{a}_k^\dagger,\hat{a}_{-k})(\boldsymbol{h}_k\cdot\boldsymbol{\sigma})\binom{\hat{a}_k}{\hat{a}_{-k}^\dagger}$, where $\boldsymbol{\sigma}$ is the Pauli vector, $\boldsymbol{h}_k=\mathbf{e}_z\cos\theta_k+\mathbf{e}_y\sin\theta_k$ is the unit Anderson vector, and $\tan\theta_k=(\Delta/2)f_\alpha(k)/(J\cos k+\mu)$. Varying k from 0 to 2π, $\boldsymbol{h}_k$ winds $W=\int_0^{2\pi}(d\theta_k/dk)(dk/2\pi)$ times in the $y-z$ plane. The schematic phase diagram of the model is shown in Fig. 1: Colored regions refer to phases with different (and constant) values of the winding number W.

For short-range pairing ($\alpha>1$), W assumes only integer values: $W=0,\pm1$. $W\neq0$ signals a topologically nontrivial phase [34], characterized by the presence of massless (Majorana) edge modes in the open chain [33]. For long-range pairing ($\alpha\le1$), semi-integer values $W=\pm1/2$ appear [39–41]. We quote the corresponding phases as "long-range": The phase for $\mu/J<1$ supports massive edge modes in the open chain, while for $\mu/J>1$ no edge mode occurs [40,41]. Long-range phases are characterized by a violation of the area law for the von Neumann entropy [17,18,42].

For $\Delta\neq0$ and in the limit $L\to\infty$, the energy gap between the superfluid ground state and the first excited state closes at $\mu/J=1$ and $k=\pi$ for all the values of α, as well as at $\mu/J=-1$ and $k=0$ when $\alpha>1$ only [see Fig. 1(a)]. Furthermore, a transition between phases with different values of the winding number W is observed when changing α at $\alpha = 1$. Remarkably, this transition occurs without closing the energy gap and is associated with various discontinuities, for instance, in the mutual information and in the decay exponents for the two-point correlations $\langle \hat{a}_i^\dagger \hat{a}_j \rangle$ and $\langle \hat{a}_i \hat{a}_j \rangle$ [17,41]. In the following, we will show that, similarly to the QPTs at $\mu/J = \pm 1$, the transitions at $\alpha = 1$ are signaled by a diverging derivative of the QFI.

Figures 1(b) and 1(c) show the phase diagram in the $\Delta/J - \mu/J$ plane for $\alpha = \infty$ and $\alpha = 0$, respectively. The energy gap closes at $\Delta = 0$ for $|\mu|/J \leq 1$ and $\cos k = -\mu/J$. For $\alpha \leq 1$ and $|\mu|/J > 1$ we have a transition—without closing the energy gap—between $W = \pm 1/2$ [39], crossing $W = 0$ on the singular line $\Delta = 0$.

Multipartite entanglement.—In the following, we witness ME in the ground state $|\psi_{\rm gs}\rangle$ of Eq. (1) using the QFI, $F_Q[|\psi_{\rm gs}\rangle, \hat{O}]$, where $\hat{O}$ is a Hermitian operator that we specify below. First, let us recall that, in general, the QFI is convex in the state and can thus be used as a ME witness [28–31]. We have that $F_Q[\sum_j p_j |\psi_j\rangle\langle\psi_j|, \hat{O}] \leq \sum_j p_j F_Q[|\psi_j\rangle, \hat{O}]$ holds for arbitrary states and operators [31], where $p_j \geq 0$ and $\sum_j p_j = 1$. Furthermore, $F_Q[|\psi\rangle, \hat{O}] = 4(\Delta\hat{O})^2_{|\psi\rangle}$ for pure states [43]. The QFI of any κ-partite entangled state $\hat{\rho}_{\kappa\text{-ent}}$ is thus bounded as $F_Q[\hat{\rho}_{\kappa\text{-ent}}, \hat{O}] \leq b_{\kappa,\hat{O}}$, where $b_{\kappa,\hat{O}} \equiv \max_{|\psi_{\kappa\text{-ent}}\rangle} 4(\Delta\hat{O})^2_{|\psi_{\kappa\text{-ent}}\rangle}$ is the maximum over all κ-partite entangled pure states [44]. Here we calculate the QFI with respect to the nonlocal operator $\hat{O}_\rho = \sum_{j=1}^L \hat{o}_\rho^{(j)}/2$ ($\rho = x, y$), where

$$\hat{o}_\rho^{(j)} = (-i)^{\delta_{\rho,y}} [\hat{a}_j^\dagger e^{i\pi \sum_{l=1}^{j-1} \hat{n}_l} + (-1)^{\delta_{\rho,y}} e^{-i\pi \sum_{l=1}^{j-1} \hat{n}_l} \hat{a}_j], \quad (3)$$

$\delta_{\rho,y} = 1$ for $\rho = y$, and $\delta_{\rho,y} = 0$ otherwise, and $\hat{n}_j = \hat{a}_j^\dagger \hat{a}_j$. This choice is suggested by the relation—via the Jordan-Wigner transform [36]—of Eq. (1) (for $\alpha = \infty$) and the Ising Hamiltonian (for nearest-neighbor interaction among spin-1/2 particles). Via Jordan-Wigner, $\hat{O}_\rho$ transforms to the order parameter of the Ising model, and it is thus characterized by a large variance in the ferromagnetic phase. It is interesting to notice (see below) that, with the same choice of the operator $\hat{O}_\rho$, we are able to detect ME also for arbitrary-range pairing ($\alpha < \infty$), where the short-range Ising and the Kitaev Hamiltonians do not map to each others. This demonstrates that our approach is not limited to the short-range Kitaev chain (which can be exactly mapped to the short-range Ising) but can be extended to study a generic topological model with the help of an "educated guess" for the choice of the operator.

For the operator $\hat{O}_\rho$, the ME bound is $b_{\kappa,\hat{O}_\rho} = s\kappa^2 + r^2$ [37], where s is the integer part of L/κ and $r = L - s\kappa$. Approximating s with L/κ, we have that the violation of the inequality

$$f_Q[|\psi_{\rm gs}\rangle, \hat{O}_\rho] \leq \kappa \quad (4)$$

signals $(\kappa + 1)$-partite entanglement $(1 \leq \kappa \leq L - 1)$ between sites of the fermionic chain, where $f_Q = F_Q/L$ is the Fisher density. In particular, separable states satisfy $f_Q \leq 1$, while $f_Q = L$ is the ultimate (Heisenberg) bound.

Finally, we point out that the QFI can be experimentally addressed: It is related to the dynamical susceptibility [25,45] (see also Refs. [46–48] regarding the detection of entanglement with similar methods), and a lower bound can be obtained from the variation of statistical distributions with the phase shift parameter θ when applying the transformation $e^{-i\theta\hat{O}}$ [31,49].

QFI phase diagram.—We have calculated the QFI for different values of the parameters of the Kitaev chain using standard exact techniques [36]. The QFI follows an asymptotic power-law scaling

$$f_Q[|\psi_{\rm gs}\rangle, \hat{O}_\rho] = 1 + cL^b, \quad (5)$$

where the coefficients b and c depend on μ/J, δ/J, α, and ρ but are independent on L. The scaling behavior is reported schematically in Fig. 1, while Fig. 2 shows numerical values of b obtained up to $L \approx 1000$.

The scaling exponent b is directly related to the behavior of the correlation function for the operator $\hat{O}_\rho$. Indeed, noticing that for the ground state of the Kitaev model $\langle\psi_{\rm gs}|\hat{O}_\rho|\psi_{\rm gs}\rangle = 0$, we can rewrite the Fisher density $f_Q[|\psi_{\rm gs}\rangle, \hat{O}_\rho] = 4\langle\psi_{\rm gs}|\hat{O}_\rho^2|\psi_{\rm gs}\rangle/L$ as

$$f_Q[|\psi_{\rm gs}\rangle, \hat{O}_\rho] = 1 + \sum_{l=1}^{L-1} C_\rho(l), \quad (6)$$

where $C_\rho(l) = \langle\psi_{\rm gs}|\hat{o}_\rho^{(1)}\hat{o}_\rho^{(1+l)}|\psi_{\rm gs}\rangle$. For instance, an exponentially decaying correlation, $C_\rho(l) = e^{-d_l/\xi}$ on a ring, with $\xi > 0$ independent on L, gives $b = 0$ and $c = 2/(e^{1/\xi} - 1)$ in the thermodynamic limit. In this case, the QFI is extensive: $c > \kappa - 1$ is obtained for $\xi^{-1} < \log[(\kappa + 1)/(\kappa - 1)]$ and witnesses κ-partite entanglement that remains constant when increasing the system size. Instead, when $b > 0$, the QFI is superextensive: The larger L is, the larger the witnessed κ-partite entanglement is. Values $0 < b < 1$ can be related to a rescaling of the correlation functions with the system size, $C_\rho(l) = L^{b-1} c_\rho(l/L)$, giving $c = \int_0^1 dx c_\rho(x)$. This is obtained, for instance, when $C(l) \sim 1/l^{1-b}$. For long-range pairing, $\Delta > 0$ and $\mu/J \geq 1$, the correlation function is staggered [37], and we witness ME by calculating the QFI with respect to the staggered operator $\hat{O}_\rho^{(\rm st)} = \sum_{j=1}^L (-1)^j \hat{o}_\rho^{(j)}/2$: a choice that maximizes the variance $(\Delta\hat{O}_\rho^{(\rm st)})^2_{|\psi_{\rm gs}\rangle}$.

In Figs. 1(a) and 2(a), we plot b in the $\mu/J - \alpha$ plane. For short-range pairing ($\alpha > 1$), we find $b = 1$ for $|\mu|/J < 1$ and $b = 0$ for $|\mu|/J > 1$: A superextensive QFI is observed

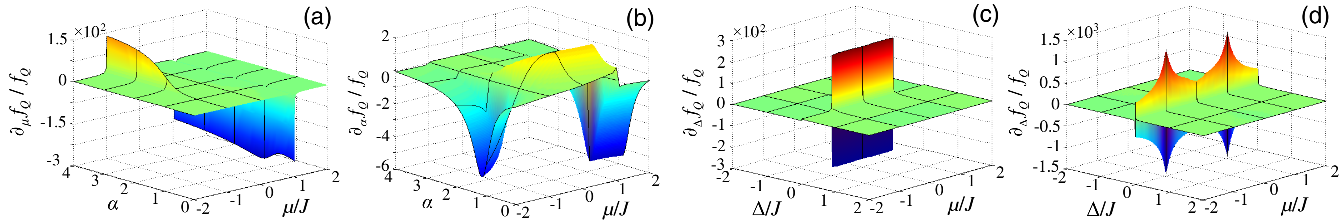

FIG. 3. Upper panels: Weighted derivative of the Fisher density, $(1/f_Q)(\partial f_Q/d\eta)$, with respect to $\eta = \mu/J$ (a), α (b), and Δ/J (c),(d). Black lines are a guide to the eye (cuts at integer values of the parameters). All plots have been obtained for $L = 1000$ sites. In (a) and (b) $\Delta = J$; in (c) $\alpha = \infty$, while in (d) $\alpha = 0$. The singularities at $\alpha = 1$ for $(1/f_Q)(\partial f_Q/d\alpha)$ (b) develop slowly in the system size; see [37] for a finite-size scaling analysis.

only in the topologically nontrivial phase. On the critical lines $|\mu|/J = 1$, we have $b = 3/4$, that is associated to the algebraic asymptotic decay of the correlation functions, $C_x(l \to L) \sim L^{1/4}$, implied at $\alpha > 2$ by conformal invariance [9,50]. For $\alpha \approx 1$, the numerical calculations are affected by finite-size effects. We argue that $b = 1/2$ for $|\mu|/J > 1$ and $b = 3/4$ for $|\mu|/J \le 1$. For long-range pairing ($\alpha < 1$), $b = 3/4$ for $\mu/J \neq 1$ and $b = 1/2$ for $\mu/J = 1$. The above scalings refer—for every α—to the QFI relative to an optimal choice of operators [51], that is, $\hat{O}_x$ for $\mu/J \le 1$ and $\hat{O}_y^{(\mathrm{st})}$ for $\mu/J \ge 1$.

In Figs. 1 and 2, we also plot b in the $\Delta/J - \mu/J$ plane for nearest-neighbor [$\alpha = \infty$, panel (b)] and infinite-range [$\alpha = 0$, panel (c)] pairings. Notice that the regime $\Delta < 0$ is mapped on the one at $\Delta > 0$ by the phase redefinition $\hat{a}_j \to \pm i\hat{a}_j$; this operation also interchanges $f_Q[|\psi_{\mathrm{gs}}\rangle, \hat{O}_x] \leftrightarrow f_Q[|\psi_{\mathrm{gs}}\rangle, \hat{O}_y]$ and $f_Q[|\psi_{\mathrm{gs}}\rangle, \hat{O}_x^{(\mathrm{st})}] \leftrightarrow f_Q[|\psi_{\mathrm{gs}}\rangle, \hat{O}_y^{(\mathrm{st})}]$. For $\alpha = \infty$ and $\Delta \neq 0$, we have $b = 1$ for $|\mu|/J < 1$, $b = 3/4$ for $|\mu|/J = 1$, and $b = 0$ elsewhere. For $|\Delta|/J = 0$ and $|\mu|/J < 1$, we have $b = 1/2$. Again, a superextensive scaling of the QFI is found in the correspondence of phases with a nonzero winding number. For $\alpha = \infty$ (when the Kitaev Hamiltonian maps to the short-range Ising model, for $\Delta = J$), our results agree with existing calculations [25,26]. In particular, the correlation function of the $\hat{O}_x$ operator is exponentially decaying for $|\mu|/J > 1$ and constant for $|\mu|/J < 1$: Genuine L-partite entanglement is witnessed at $\mu = 0$ where $C_x(l) = 1 \forall l$ [37]. For $\Delta = 0$ (and every α), the Kitaev chain maps to the XX model. It is known [52] that the ground state is a product state for $|\mu|/J > 1$, and, accordingly, we find $c = 0$ in this case [37]. In the full diagram of Fig. 2(b), the optimal choice of operators is $\hat{O}_x$ for $\Delta/J \ge 0$ and $\hat{O}_y$ for $\Delta/J \le 0$. For infinite-range pairing ($\alpha = 0$), we find $b = 3/4$ everywhere, except at the phase boundaries: $b = 1/2$ for $\mu/J = 1$ and $\Delta \neq 0$, as well as for $\Delta = 0$ and $|\mu|/J < 1$, while $b = 0$ for $\Delta = 0$ and $|\mu|/J \ge 1$. We can distinguish four regions in the phase diagram of Fig. 2(c), singled out by the operators optimizing the QFI. For $\mu/J < 1$, the optimal operators [51] are $\hat{O}_x$ for $\Delta > 0$ and $\hat{O}_y$ for $\Delta < 0$, while, if $\mu/J > 1$, they are $\hat{O}_y^{(\mathrm{st})}$ for $\Delta > 0$ and $\hat{O}_x^{(\mathrm{st})}$ for $\Delta < 0$.

Next, we show that the transition between phases characterized by different values of the winding number W is signaled by a diverging derivative of the QFI. This is illustrated in Fig. 3, where we plot the weighted derivative of f_Q with respect to μ/J [panel (a)], α [panel (b)], and Δ/J [panels (c) and (d)]. These results can be understood by taking the derivative of Eq. (5) with respect to a parameter η of the model (i.e., $\eta = \mu/J$, Δ/J, or α):

$$\frac{1}{f_Q}\frac{\partial f_Q}{\partial \eta} = \frac{cL^b}{1 + cL^b} \times \left(\frac{1}{c}\frac{\partial c}{\partial \eta} + \frac{\partial b}{\partial \eta}\log L\right). \tag{7}$$

In the interesting case $c \neq 0$ and $b \ge 0$, Eq. (7) diverges in the thermodynamic limit $L \to \infty$ either because of a divergence of $\partial_\eta c/c$ or, even when $\partial_\eta c$ is smooth, because of $\partial_\eta b \neq 0$. Figure 3, obtained at $L = 1000$, shows that, while $\partial_\mu f_Q/f_Q$ and $\partial_\Delta f_Q/f_Q$ vary sharply at the phase transition points in Fig. 1 (see [37] for a plot of the coefficients b and c), $\partial_\alpha f_Q/f_Q$ varies smoothly as a function α. Yet, a finite-size scaling analysis [37] shows that, in the limit $L \to \infty$ (up to $L = 5000$ in our numerics), $\partial_\alpha f_Q/f_Q$ tends to peaks at $\alpha = 1$. Therefore, a fast change of the QFI is able to detect the transition at $\alpha = 1$—associated to a change of the winding number—even if it occurs without closing the energy gap in the quasiparticle spectrum. We notice here that the fidelity susceptibility [53,54] has a similar behavior [55].

Conclusions.—The quantum Fisher information detects multipartite entanglement in the topological and long-range phases (with nonvanishing winding numbers) of the Kitaev chain with variable-range pairing. A key aspect is the calculation of the quantum Fisher information relative to nonlocal operators showing long-range correlations, whereas the quantum Fisher information relative to local operators is unable to detect entanglement in this model, as noted in Ref. [25].

Furthermore, QPTs are identified by the divergence of the derivative of the quantum Fisher information with respect to different control parameters, even when the phase transition is not associated to a closing gap in the excitation spectrum. Our results are a step forward in the study of entanglement in topological superconductors by providing a clear evidence of multipartite entanglement in these systems.

We thank S. Ciuchi, S. Paganelli, and D. Vodola for useful discussions.

[1] L. Amico, R. Fazio, A. Osterloh, and V. Vedral, Entanglement in many-body systems, Rev. Mod. Phys. **80**, 517 (2008).
[2] B. Zeng, X. Chen, D.-L. Zhou, and X.-G. Wen, Quantum information meets quantum matter, arXiv:1508.02595.
[3] R. Horodecki, P. Horodecki, M. Horodecki, and K. Horodecki, Quantum entanglement, Rev. Mod. Phys. **81**, 865 (2009).
[4] O. Gühne and G. Tòth, Entanglement detection, Phys. Rep. **474**, 1 (2009).
[5] F. Verstraete, M. Popp, and J. I. Cirac, Entanglement versus Correlations in Spin Systems, Phys. Rev. Lett. **92**, 027901 (2004).
[6] T. J. Osborne and M. A. Nielsen, Entanglement in a simple quantum phase transition, Phys. Rev. A **66**, 032110 (2002).
[7] A. Osterloh, L. Amico, G. Falci, and R. Fazio, Scaling of entanglement close to a quantum phase transition, Nature (London) **416**, 608 (2002).
[8] S. Sachdev, *Quantum Phase Transitions* (Cambridge University Press, Cambridge, England, 1999).
[9] G. Mussardo, *Statistical Field Theory, An Introduction to Exactly Solvable Models in Statistical Physics* (Oxford University Press, New York, 2010).
[10] J. Eisert, M. Cramer, and M. Plenio, Area laws for the entanglement entropy, Rev. Mod. Phys. **82**, 277 (2010).
[11] F. Verstraete, M. Popp, J. I. Cirac, F. G. S. L. Brandao, and M. Horodecki, An area law for entanglement from exponential decay of correlations, Nat. Phys. **9**, 721 (2013).
[12] F. G. S. L. Brandao and M. Cramer, Entanglement area law from specific heat capacity, Phys. Rev. B **92**, 115134 (2015).
[13] J. I. Latorre and A. Riera, A short review on entanglement in quantum spin systems, J. Phys. A **42**, 504002 (2009).
[14] G. Vidal, J. I. Latorre, E. Rico, and A. Kitaev, Entanglement in Quantum Critical Phenomena, Phys. Rev. Lett. **90**, 227902 (2003).
[15] P. Calabrese and J. Cardy, Entanglement entropy and quantum field theory, J. Stat. Mech. (2004) P06002.
[16] T. Koffel, M. Lewenstein, and L. Tagliacozzo, Entanglement Entropy for the Long-Range Ising Chain in a Transverse Field, Phys. Rev. Lett. **109**, 267203 (2012).
[17] D. Vodola, L. Lepori, E. Ercolessi, A. V. Gorshkov, and G. Pupillo, Kitaev Chains with Long-Range Pairing, Phys. Rev. Lett. **113**, 156402 (2014).
[18] F. Ares, J. G. Esteve, F. Falceto, and A. R. de Queiroz, Entanglement in fermionic chains with finite-range coupling and broken symmetries, Phys. Rev. A **92**, 042334 (2015).
[19] D. Vodola, L. Lepori, E. Ercolessi, and G. Pupillo, Long-range Ising and Kitaev models: Phases, correlations and edge modes, New J. Phys. **18**, 015001 (2016).
[20] R. Movassagh and P. W. Shor, Supercritical entanglement in local systems: Counterexample to the area law for quantum matter, Proc. Natl. Acad. Sci. U.S.A. **113**, 13278 (2016).
[21] L.-A. Wu, M. S. Sarandy, and D. A. Lidar, Quantum Phase Transitions and Bipartite Entanglement, Phys. Rev. Lett. **93**, 250404 (2004).
[22] O. Gühne, G. Tòth, and H. J. Briegel, Multipartite entanglement in spin chains, New J. Phys. **7**, 229 (2005).
[23] M. Hofmann, A. Osterloh, and O. Gühne, Scaling of genuine multiparticle entanglement close to a quantum phase transition, Phys. Rev. B **89**, 134101 (2014).
[24] J. Stasinska, B. Rogers, M. Paternostro, G. De Chiara, and A. Sanpera, Long-range multipartite entanglement close to a first-order quantum phase transition, Phys. Rev. A **89**, 032330 (2014).
[25] P. Hauke, M. Heyl, L. Tagliacozzo, and P. Zoller, Measuring multipartite entanglement through dynamic susceptibilities, Nat. Phys. **12**, 778 (2016).
[26] W.-F. Liu, J. Ma, and X. Wang, Quantum Fisher information and spin squeezing in the ground state of the XY model, J. Phys. A **46**, 045302 (2013).
[27] J. Ma and X. Wang, Fisher information and spin squeezing in the Lipkin-Meshkov-Glick model, Phys. Rev. A **80**, 012318 (2009).
[28] L. Pezzè and A. Smerzi, Entanglement, Nonlinear Dynamics, and the Heisenberg Limit, Phys. Rev. Lett. **102**, 100401 (2009).
[29] P. Hyllus, W. Laskowski, R. Krischek, C. Schwemmer, W. Wieczorek, H. Weinfurter, L. Pezzè, and A. Smerzi, Fisher information and multiparticle entanglement, Phys. Rev. A **85**, 022321 (2012).
[30] G. Tóth, Multipartite entanglement and high-precision metrology, Phys. Rev. A **85**, 022322 (2012).
[31] L. Pezzè, Y. Li, W. Li, and A. Smerzi, Witnessing entanglement without entanglement witness operators, Proc. Natl. Acad. Sci. U. S. A. **113**, 11459 (2016).
[32] A. P. Schnyder, S. Ryu, A. Furusaki, and A. W. W. Ludwig, Classification of topological insulators and superconductors, AIP Conf. Proc. **1134**, 10 (2009).
[33] A. Y. Kitaev, Unpaired Majorana fermions in quantum wires, Phys. Usp. **44**, 131 (2001).
[34] J. Alicea, New directions in the pursuit of Majorana fermions in solid state systems, Rep. Prog. Phys. **75**, 076501 (2012).
[35] A. Alecce and L. Dell'Anna, Extended Kitaev chain with longer range hopping and pairing, Phys. Rev. B **95**, 195160 (2017).
[36] E. Lieb, T. Schultz, and D. Mattis, Two soluble models of an antiferromagnetic chain, Ann. Phys. (N.Y.) **16**, 407 (1961).
[37] See Supplemental Material at http://link.aps.org/supplemental/10.1103/PhysRevLett.119.250401 for a discussion of: (i) the Hamiltonian (1) and basic equations; (ii) quantum Fisher information and multipartite entanglement; (iii) correlation functions and polynomial fits; (iv) finite-size scaling analysis around $\alpha = 1$.
[38] In the case $\Delta < 0$, the phase diagram is obtained by changing $W \to -W$.
[39] These fractional numbers are due to the singularity of $f_\alpha(k)$ for $\alpha < 1$ that occurs at $k = 0, 2\pi$ in the thermodynamic limit and do not testify the topological stability, nor the presence of edge modes, in general [40, 41]. Specifically, massive edge states are found for $\mu/J < 1$ for both $\Delta > 0$ (a phase characterized by $W = 1/2$) and $\Delta < 0$ (a phase characterized by $W = -1/2$). See also K. Patrick, T. Neupert, and J. K. Pachos, Topological Quantum Liquids with Long-Range Couplings, Phys. Rev. Lett. **118**, 267002 (2017).
[40] O. Viyuela, D. Vodola, G. Pupillo, and M. A. Martin-Delgado, Topological massive Dirac edge modes and long-range superconducting Hamiltonians, Phys. Rev. B **94**, 125121 (2016).

[41] L. Lepori and L. Dell'Anna, Long-range topological insulators and weakened bulk-boundary correspondence, New J. Phys. **19**, 103030 (2017).

[42] L. Lepori, D. Giuliano, and S. Paganelli, Edge insulating topological phases in a two-dimensional long-range superconductors, arXiv:1707.0577.

[43] General expressions for the QFI and a review of its properties can be found in L. Pezzè and A. Smerzi, in *Atom Interferometry, Proceedings of the International School of Physics "Enrico Fermi", Course 188, Varenna*, edited by G. M. Tino and M. A. Kasevich (IOS Press, Amsterdam, 2014), p. 691 [arXiv:1411.5164].

[44] We recall that a pure state is κ-partite entangled if it can be written as the product $|\psi_{\kappa\text{-ent}}\rangle = \otimes_j |\psi_j\rangle$, where $|\psi_j\rangle$ is a state of $L_j \leq \kappa$ parties and $\sum_j L_j = L$. κ-partite entangled states form a convex set [4].

[45] I. Frérot and T. Roscilde, Quantum variance: A measure of quantum coherence and quantum correlations for many-body systems, Phys. Rev. B **94**, 075121 (2016).

[46] M. Cramer, M. B. Plenio, and H. Wunderlich, Measuring Entanglement in Condensed Matter Systems, Phys. Rev. Lett. **106**, 020401 (2011).

[47] P. Krammer, H. Kampermann, D. Bruss, R. A. Bertlmann, L. C. Kwek, and C. Macchiavello, Multipartite Entanglement Detection via Structure Factors, Phys. Rev. Lett. **103**, 100502 (2009).

[48] O. Marty, M. Epping, H. Kampermann, D. Bru, M. B. Plenio, and M. Cramer, Quantifying Entanglement with Scattering Experiments, Phys. Rev. Lett. **89**, 125117 (2014).

[49] H. Strobel, W. Muessel, D. Linnemann, T. Zibold, D. B. Hume, L. Pezzè, A. Smerzi, and M. K. Oberthaler, Fisher information and entanglement of non-Gaussian spin states, Science **345**, 424 (2014).

[50] L. Lepori, D. Vodola, G. Pupillo, G. Gori, and A. Trombettoni, Effective theory and breakdown of conformal symmetry in a long-range quantum chain, Ann. Phys. (Amsterdam) **374**, 35 (2016).

[51] In practice, for every different parameter in Eq. (1) we calculate the QFI with respect to the four operators $\hat{O}_\rho$ and $\hat{O}_\rho^{(\mathrm{st})}$ ($\rho = x, y$). The scaling exponent b in Figs. 1 and 2 refers to the largest of such four QFI.

[52] E. Barouch and B. M. McCoy, Statistical mechanics of the XY model. II. Spin correlation functions, Phys. Rev. A **3**, 786 (1971).

[53] W.-L. You, Y.-W. Li, and S.-J. Gu, Fidelity, dynamic structure factor, and susceptibility in critical phenomena, Phys. Rev. E **76**, 022101 (2007).

[54] P. Zanardi, P. Giorda, and M. Cozzini, Information-Theoretic Differential Geometry of Quantum Phase Transitions, Phys. Rev. Lett. **99**, 100603 (2007); M. Cozzini, P. Giorda, and P. Zanardi, Quantum phase transitions and quantum fidelity in free fermion graphs, Phys. Rev. B **75**, 014439 (2007); P. Zanardi, L. Campos Venuti, and P. Giorda, Bures metric over thermal state manifolds and quantum criticality, Phys. Rev. A **76**, 062318 (2007).

[55] L. Pezzè *et al.* (to be published).